Asociación Argentina
de Mecánica Computacional

Mecánica Computacional Vol XXXVIII, págs. 259-268 (artículo completo)
H.G. Castro, J.L. Mroginski, R.R. Paz, M.A. Storti (Eds.)
Resistencia, 1-5 Noviembre 2021

STIFFNESS MATRIX FOR A BATTENED BEAM INCLUDING SHEAR EFFECTS

Claudio E. Jouglard and Uri Peker

Departamento de Ingeniería Civil, Facultad Regional Buenos Aires, Universidad Tecnológica Nacional, Mozart 2300, C1407IVT Buenos Aires, Argentina, claudio.jouglard@frba.utn.edu.ar, http://www.frba.utn.edu.ar

Keywords: Battened Beams, Finite Elements, Simplified Stiffness Matrix, Shear Deformation.

Abstract. A battened beam is composed of chords and battens. The model of a structure composed by this type of beams is done, generally, by modeling each batten and chord sectors between battens using beam finite elements, and this implies models with a large number of degrees of freedom. In the previous stages of design or to do simple verifications is convenient to have a simplified analytical solution to assimilate the lattice beam to an equivalent solid beam. To do this we consider a pattern of bars that repeats many times along the beam and using variational techniques it is possible to find an approximated continuous formulation for the displacements of the beam. The shear effects must be taken into account to reproduce adequately the case of very stiff battens where the influence of the shear effect is important. The purpose of this work is to obtain a simplified stiffness matrix for a finite element of a battened beam. These finite elements can be incorporated into a finite element program to obtain approximate solutions in frames. Comparisons are made with the complete finite element solution that show a very good approximation.

1 INTRODUCTION

Lattice structures are very useful since they can cover large spans without intermediate supports. In addition, their low weight and ease of folding and assembly make them ideal for aerospace applications. This type of structures began to be studied with intensity in the 1970s (Noor, 1988). They are also used in antenna support structures (Guzmán, 2014; Martín, 2017) and currently in the design of new materials (Helou and Kara, 2018) whose microstructure exhibits a repetitive pattern of interconnected bars.

The methods of analysis of lattice structures can be grouped into four classes (Noor, 1988): 1) direct methods, 2) discrete field methods, 3) periodic structure methods and 4) continuous medium analogy.

In a direct method the structure is analyzed by finite elements and each bar is modeled individually. In the discrete field methods it is assumed that the structure has a certain regularity and equations of equilibrium or energy are writing at a typical node of the lattice beam and the resulting difference equations are solved directly or using truncated Taylor series expansions to replace the difference equations by differential equations. In periodic structure methods, finite elements are combined with transfer matrices to reduce the degrees of freedom involved, although the solution is purely numerical. Finally, using the analogy of the continuous medium, the lattice beam is replaced by an equivalent continuous model.

Currently the modeling of the lattice beams is carried out by finite elements using one element per bar, which leads a large number of degrees of freedom. This makes the analysis of these structures computationally expensive, especially if the analysis is non-linear, as recommended by current regulations. Then it is convenient to replace the lattice beam with an equivalent solid beam to reduce the degrees of freedom.

The behavior of a lattice girder is quite similar to that of a solid beam, although it exhibits greater shear deformation due to the flexibility of the lattices.

A first simplification could be to approximate the lattice beam by a solid beam with the same inertia and area, but this ignores the shear strains, that can be large for flexible lattice beams. Considering the shear deformations of the lattice beam as a solid beam can gives good results but in some cases this approximation does not reflects the true behavior of the lattice beam, as we will see in the examples.

Among the local references we can mention (Filipich and Bambill, 2003; Filipich et al., 2010; Guzmán et al., 2019; Guzmán, 2014; Martín, 2017; Maurizi et al., 2004), where various structures are analyzed in lattice, in particular, applied to antenna masts.

Previously, in the reference (Jouglard and Peker, 2019), battened beams were analyzed using a discrete field method to obtain a system of equivalent differential equations whose solution was obtained analytically and good approximations to the stiffness matrix were obtained. However, the distortion produced by shear deformations, which are important in the case of very rigid battens, was not considered.

This was improved in the reference (Jouglard, 2020), where equivalent differential equations were derived considering shear distortion and good approximations were obtained for the stiffness matrix and vertical displacements and rotations. In that work, the Rayleigh-Ritz method (Rektorys, 1980) was used with polynomial approximations of the displacements, although a linear variation was considered for the horizontal displacements that is insufficient to obtain a good approximation of the displacements and were corrected in this work.

The paper is organized as follows, firstly we present the equivalent beam model and the deduction of the equivalent stiffness matrix for the battened beam. Finally, we show some numerical examples.

2 MODEL DESCRIPTION

Let us consider a battened beam composed of two longitudinal bars (chords) of length L and evenly spaced vertical battens. We define a local x, y coordinate system with origin at the left edge.

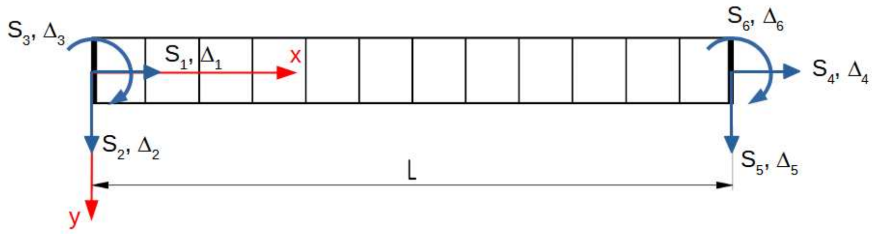

Figure 1: Beam model

Assuming that the supports of the beam are undeformable so their movements can be described by two translations and one rotation that we will refer to the midpoint of each end. We will call $\Delta_1, \Delta_2, \Delta_3$ the translation according to x, translation according to y and rotation of the left end, respectively, and $\Delta_4, \Delta_5, \Delta_6$ the corresponding generalized displacements of the right end. In correspondence with the generalized displacements Δ_i of each end, we will have generalized forces S_i acting in the same directions, as shown in Figure 1.

Furthermore, we consider that the two chords are equal and have area A_l and inertia J_l. The vertical battens of height h are spaced a distance d and have area A_p and inertia J_p. The chords have modulus of elasticity E_l and the battens E_p.

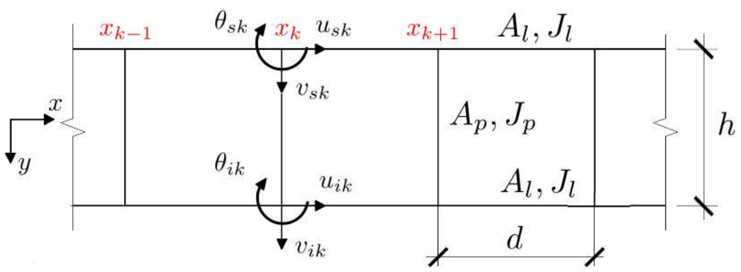

Figure 2: Beam sector

The internal joints are assumed rigid and therefore during the deformation a node k of the beam moves with translations u_k, v_k in the x, y directions and undergoes a rotation θ_k in the plane. We will call $u_{sk}, v_{sk}, \theta_{sk}$ to the nodal displacements of the node k of the upper chord and $u_{ik}, v_{ik}, \theta_{ik}$ for the node k of the lower chord (see Figure 2).

If the chords are flexible, a shear distortion effect can occur, as shown in Figure 3. This effect is equivalent to that of shear deformation in solid beams and is represented by an additional shear rotation.

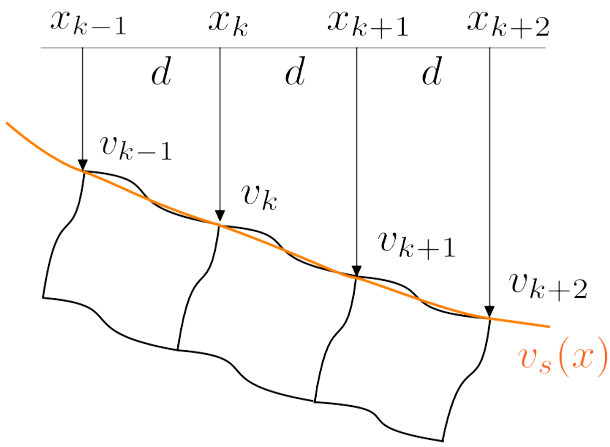

Figure 3: Shear distortion

We will assume that the displacements and rotations of each node can be approximated by means of continuous functions $u_s(x), v_s(x), \theta_s(x)$ for the upper chord and $u_i(x), v_i(x), \theta_i(x)$ for the lower chord.

Then the nodal displacements of node k are

$$\begin{array}{ll} u_{sk} \approx u_s(x_k) & u_{ik} \approx u_i(x_k) \\ v_{sk} \approx v_s(x_k) & v_{ik} \approx v_i(x_k) \\ \theta_{sk} \approx \theta_s(x_k) & \theta_{sk} \approx \theta_i(x_k) \end{array} \tag{1}$$

If we analyze the nodal rotations at the upper chord we can distinguish three rotation angles (Figure 4): θ_s which is the physical rotation of the node in the plane of the beam, 2) ϕ_s which is the flexural rotation due to transverse displacements and 3) ψ_s which is the rotation by distortion or shear.

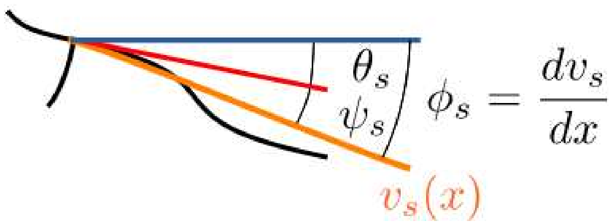

Figure 4: Nodal rotations

The angle ϕ_s between the horizontal and the tangent of the transverse displacements $v_s(x)$ can be approximated, for small displacements, by the derivative of the displacement function $v_s(x)$ resulting

$$\phi_s = \frac{dv_s}{dx} \tag{2}$$

The distortion angle ψ_s, which would be the equivalent of shear distortion in a solid beam, is obtained by the difference between the flexural and the physical rotations as:

$$\psi_s = \frac{dv_s}{dx} - \theta_s \tag{3}$$

Note that, as shown in Figure 3, the function $v_s(x)$ does not represent the true displacements of the chord, but only the vertical displacements at the nodes.

3 ENERGY OF DEFORMATION

The deformation energy of a system is made up of the sum of the energies of its deformable parts. Therefore, for a battened beam, its deformation energy U will be composed of the deformation energies U_s and U_i of the upper and lower chords and by the deformation energy U_p of the battens

$$U = U_s + U_i + U_p \tag{4}$$

where these energies will be obtained by adding the deformation energies of each bar and we will assume that each bar is slender, that is, the shear deformations in each bar can be neglected, and we will consider that all joints are rigid.

3.1 Energy of deformation of the battens

We will call U_{pk} to the deformation energy of a batten located at a distance x_k from the left support. The deformation energy will be the sum of the energies of each batten and assuming that there are a large number of battens and that the separation d is small with respect to the length L we have:

$$U_p = \sum_k U_{pk} \approx \frac{1}{d}\int_0^L U_{pk}(x)dx \tag{5}$$

Then considering only bending and axial deformations the energy of deformation of the battens is

$$\begin{aligned} U_p = \int_0^L \Bigg[& \frac{E_pA_p}{2dh}(v_i - v_s)^2 + \frac{6E_pJ_p}{dh^3}(u_i - u_s)^2 \\ & + \frac{6E_pJ_p}{dh^2}(u_i - u_s)\big(v_s' + v_i' - \psi_s - \psi_i\big) \\ & + \frac{2E_pJ_p}{dh}\big((v_s' - \psi_s)^2 + (v_s' - \psi_s)(v_i' - \psi_i) + (v_i' - \psi_i)^2\big)\Bigg] dx \end{aligned} \tag{6}$$

3.2 Energy of deformation of the chords

We will call U_{sk}, U_{ik} to the deformation energy of an upper and lower chord sector located between joints at distance x_k and x_{k+1} from the left support. Then considering only bending and axial deformations the energy of deformation of the upper chord is

$$U_s = \int_0^L \left[\frac{E_lA_l}{2}(u_s')^2 + \frac{E_lJ_l}{2}(v_s'')^2 + \frac{6E_lJ_l}{d^2}(\psi_s)^2\right] dx \tag{7}$$

Analogously for the lower chord we have

$$U_i = \int_0^L \left[\frac{E_lA_l}{2}(u_i')^2 + \frac{E_lJ_l}{2}(v_i'')^2 + \frac{6E_lJ_l}{d^2}(\psi_i)^2\right] dx \tag{8}$$

Where we have assumed that displacements at joint $k+1$ of the upper chord can be approximated from displacements at joint k as

$$u_{sk+1} \approx u_{sk} + u'_{sk} d \tag{9a}$$

$$v_{sk+1} \approx v_{sk} + v'_{sk} d + v''_{sk} \frac{d^2}{2} \tag{9b}$$

$$v'_{sk+1} \approx v'_{sk} + v''_{sk} d \tag{9c}$$

$$\psi_{sk+1} \approx \psi_{sk} \tag{9d}$$

This implies that, for an infinitesimal length d, the longitudinal displacements $u_s(x)$ are assumed linear, the transverse displacements $v_s(x)$ are assumed quadratic and the shear distortion $\psi_s(x)$ is assumed constant. A similar approximation has been made for the lower chord.

4 STIFFNESS MATRIX DERIVATION USING THE RAYLEIGH-RITZ METHOD

To obtain the equivalent stiffness matrix of the battened beam that relates the generalized forces S_i acting in the extremes with the generalized displacements Δ_i at each end (see Figure 1) we must find the solutions $u_s(x), v_s(x), \psi_s(x)$ and $u_i(x), v_i(x), \psi_i(x)$ to the differential equations of equilibrium for an unloaded beam and subjected to generalized displacements Δ_i in the supports.

Alternatively, we can use the Rayleigh-Ritz method to obtain an approximate solution. This method requires knowledge of the total potential energy V of the system

$$V = U_s + U_i + U_p - W_S \tag{10}$$

where W_S is the work of the generalized forces given as

$$W_S = \sum S_i \Delta_i = S_1\Delta_1 + S_2\Delta_2 + S_3\Delta_3 + S_4\Delta_4 + S_5\Delta_5 + S_6\Delta_6 \tag{11}$$

In this method approximated displacement functions are proposed, which depends on unknown constants c_i and the total potential energy $V(c_i)$ is minimized with respect to these constants.

4.1 Approximated displacements

We propose the next displacements approximations of the joints of the battened beam

$$\begin{aligned} \psi_s(\eta) &= c_1 & \psi_i(\eta) &= c_2 \\ u_s(\eta) &= (c_5 + c_6\eta + c_3\eta^2)L & u_i(\eta) &= (c_7 + c_8\eta + c_4\eta^2)L \\ v_s(\eta) &= (c_9 + c_{10}\eta + c_{11}\eta^2 + c_{12}\eta^3)L & v_i(\eta) &= (c_{13} + c_{14}\eta + c_{15}\eta^2 + c_{16}\eta^3)L \end{aligned} \tag{12}$$

where not all the constants c_i are free, because these functions must satisfy the boundary conditions. The details of the solution procedure can be found in reference (Jouglard, 2021).

5 STIFFNESS MATRIX OF THE BATTENED BEAM

The stiffness matrix $\mathbf{K}$ relates the generalized displacements Δ_i with the generalized forces S_i in matrix form as

$$\mathbf{K} \cdot \mathbf{\Delta} = \mathbf{S} \tag{13}$$

The coefficients k_{ij} of the stiffness matrix are obtained as

$$k_{ij} = \left.\frac{\partial^2 U}{\partial \Delta_i \partial \Delta_j}\right|_{\Delta_k=0} = \left.\frac{\partial^2 U}{\partial \Delta_j \partial \Delta_i}\right|_{\Delta_k=0} = k_{ji} \tag{14}$$

After substitution of the displacements (12) in the potential energy V and deriving with respect to the constants c_i we obtain the stiffness coefficients $k_{ij} = k_{ji}$

$$\begin{aligned}
k_{11} &= -k_{14} = k_{44} = 2\frac{E_l A_l}{L} \\
k_{22} &= -k_{25} = k_{55} = \frac{8E_p J_p}{5dhL}\alpha_3^2 + \frac{24 E_l J_l}{L^3}\alpha_4 + \frac{8E_l A_l}{3L}\alpha_2^2 \\
k_{23} &= k_{26} = -k_{35} = -k_{56} = \frac{4E_p J_p}{5dh}\alpha_3^2 + \frac{12 E_l J_l}{L^2}\alpha_4 + \frac{4E_l A_l}{3}\alpha_2^2 \\
k_{33} &= k_{66} = \frac{2E_p J_p L}{5dh}\alpha_3^2 + \frac{2E_l J_l}{L}(3\alpha_4 + 1) + \frac{E_l A_l h^2}{6L}\alpha_5 \\
k_{36} &= \frac{2E_p J_p L}{5dh}\alpha_3^2 + \frac{2E_l J_l}{L}(3\alpha_4 - 1) + \frac{E_l A_l h^2}{6L}\alpha_6
\end{aligned} \tag{15}$$

where the non-dimensional coefficients $\alpha_3, \alpha_4, \alpha_5, \alpha_6$ are

$$\begin{aligned}
\alpha_3 &= 3(1-2\alpha_1) - 2\left(\frac{L}{h}\right)\alpha_2 \qquad & \alpha_4 &= (1-2\alpha_1)^2 + 4\alpha_1^2\left(\frac{L}{d}\right)^2 \\
\alpha_5 &= 4\left(\frac{L}{h}\right)^2\alpha_2^2 + 3 \qquad & \alpha_6 &= 4\left(\frac{L}{h}\right)^2\alpha_2^2 - 3
\end{aligned} \tag{16}$$

and the coefficients α_1, α_2 are given by

$$\alpha_1 = \left(\frac{1}{2}\right)\frac{5s_1 + 3s_2 + 12}{(5s_1 + 12)(r_1^2 + 1) + 3s_2} \tag{17a}$$

$$\alpha_2 = \frac{18 r_2}{(5s_1 + 12)(r_1^2 + 1) + 3s_2} \tag{17b}$$

and where the non-dimensional coefficients s_1, s_2, r_1, r_2 are

$$\begin{aligned}
s_1 &= \frac{E_l A_l h^3 d}{E_p J_p L^2} \qquad & r_1 &= \frac{L}{d} \\
s_2 &= \frac{A_l h^2}{J_l} \qquad & r_2 &= \frac{Lh}{d^2}
\end{aligned} \tag{18}$$

6 NUMERICAL EXAMPLE

In this example we analize a battened beam of length $L = 8\ m$, height $h = 1\ m$ and separation between battens $d = 0.5\ m$. This beam has been modeled by finite elements using one finite element per batten and chord sector. The chords and battens are cylindrical bars .

To study the influence of the ratio of stiffness between chords and battens we have considered three cases: 1) flexible battens, 2) equal stiffness for chords and battens and 3) stiff battens. For the first case we have adopted cylindrical chords of 4 *in* diameter and cylindrical battens of 0.5 *in* diameter. For the second case all bars are considered cylindrical with 4 *in* diameter. And for the last case the chords have 0.5 *in* diameter and the battens have 4 *in* diameter.

We have imposed a unit vertical displacement $\Delta_2 = 1$ *mm* on the left support and the other displacements Δ_i are assumed nulls. The deformed shape of the lattice beam can be seen in Figure 5 for the extreme cases of flexible and stiff battens:

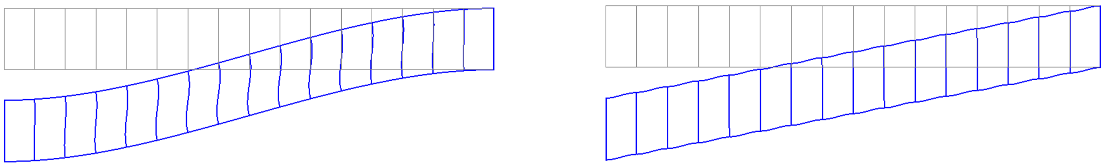

(a) flexible battens (b) stiff battens

Figure 5: Deformed shape

In the case of flexible battens (Figure 5a) the deformed shape is similar to that of a solid beam and in the case of stiff battens (Figure 5b) the deformed shape is dominated by shear where the battens only move vertically and remain almost undeformed.

If we compare the vertical displacements with those obtained by finite elements we obtain the results shown in Figure 6:

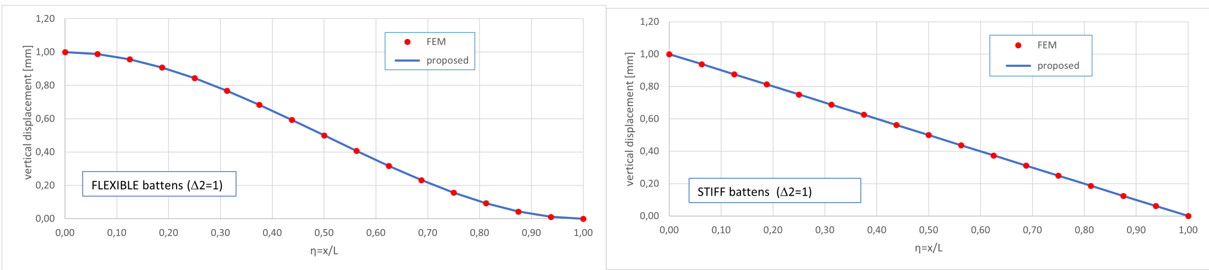

(a) flexible battens (b) stiff battens

Figure 6: Nodal vertical displacements

We note the good correlation between the vertical displacements at joints obtained by finite elements and indicated by dots and the proposed displacements represented by the solid line. If we compare the physical rotation θ_s at the joints with those obtained by finite elements we obtain the results shown in Figure 7. Again there is a good correlation between the physical rotations at joints obtained by finite elements and the proposed ones.

Although, in these two extreme cases the results of the proposed approximation are very good, when the stiffness of the battens is equal to the stiffness of the chords there are some differences in nodal displacements and rotations as shown in Figure 8:

The main reason for these discrepancies is the adopted variation for the shear distortion rotation ψ which has been considered constant in the equivalent beam model and in Figure 9 is compared with the *exact* shear distortion obtained from the finite element model.

Note that the *exact* shear distortion rotation is almost constant in the central part of the beam but increases near both ends. Also in this figure we have shown the flexural rotation which in the ends is equal to the shear distortion since the physical rotations are null in both ends.

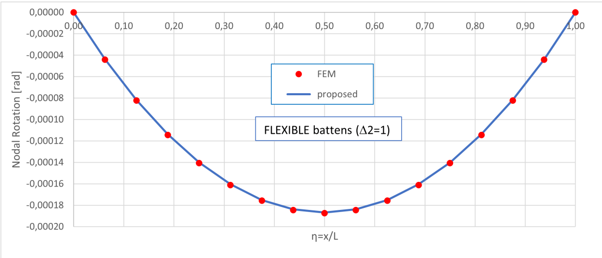

(a) flexible battens

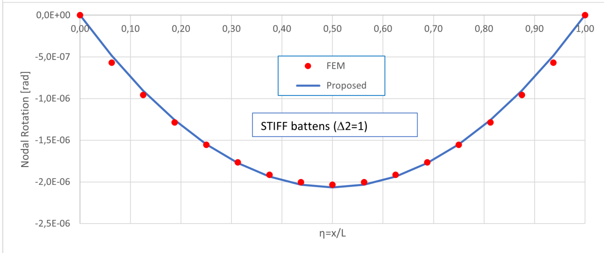

(b) stiff battens

Figure 7: Nodal physical rotations

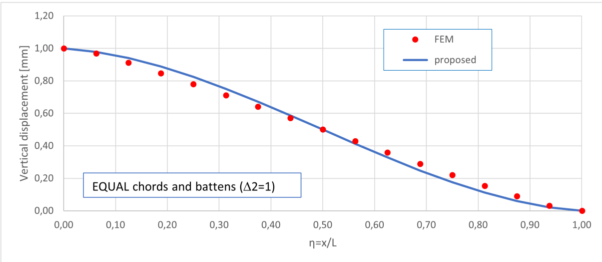

(a) nodal displacements

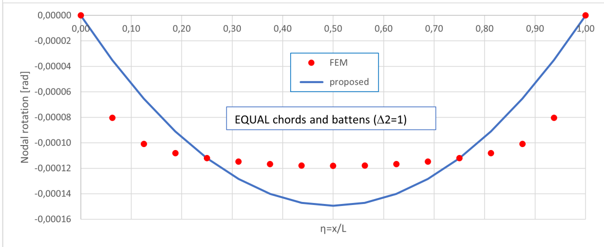

(b) nodal rotations

Figure 8: Displacements and rotations for equal stiffness of chords and battens

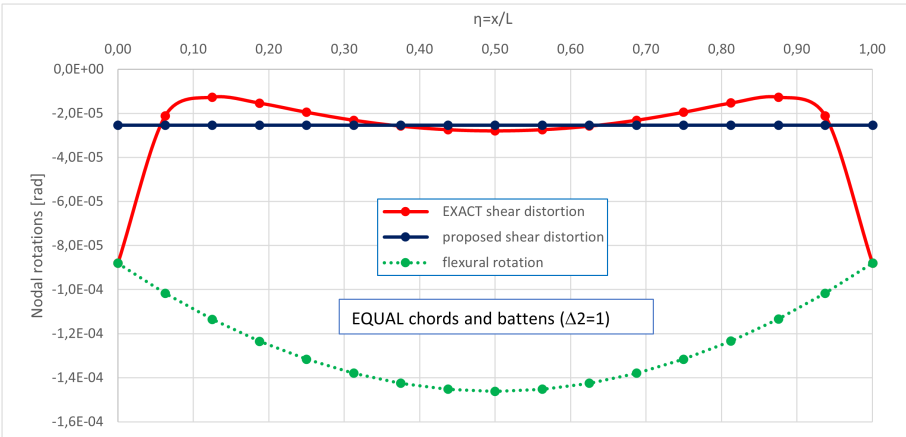

Figure 9: Comparisons of nodal rotations

7 CONCLUSIONS

An equivalent finite element stiffness matrix for a battened beam has been presented. The formulation lets to a considerable reduction in degrees of freedom and shows an excellent agreement with finite element results in extreme cases, that is, with very stiff or very flexible battens, but some differences appear when the battens and chords have the same stiffness. The main reason is the poor approximation of the shear distortion, that has been considered constant in the model. This can be improved adopting a higher degree polynomial (at least six degree) for the shear distortion but it can be cumbersome and difficult to solve. Another possibility is to derive an analytical solution, like that shown in reference (Jouglard and Peker, 2019).

REFERENCES

Cook R.D., Malkus D.S., Plesha M.E., and Witt R.J. *Concepts and Applications of Finite Element Analysis*. Wiley, 4th edition, 2001. ISBN 978-0-471-35605-9.

Filipich C.P. and Bambill E.A. Frecuencias Naturales De Piezas Empresilladas Via Series De Potencias. *Mecánica Computacional*, 22(10):877–891, 2003.

Filipich C.P., Guzmán A.M., and Rosales M.B. Planteo Discreto-Continuo de Piezas Reticuladas Planas y Espaciales. *Mecánica Computacional*, 29(9):863–882, 2010.

Guzmán A.M., Rosales M.B., and Filipich C.P. Continuous one-dimensional model of a spatial lattice. Deformation, vibration and buckling problems. *Engineering Structures*, 182:290–300, 2019.

Guzmán A.M. *Estática, Estabilidad y Dinámica de Mástiles Reticulados con Aplicación a Estructuras Arriostradas*. Tesis de Doctorado, Universidad Nacional del Sur, Bahía Blanca, Argentina, 2014.

Helou M. and Kara S. Design, analysis and manufacturing of lattice structures: an overview. *International Journal of Computer Integrated Manufacturing*, 31(3):243–261, 2018.

Jennings A. *Matrix Computation for Engineers and Scientists*. John Wiley & Sons, 1977.

Jouglard C.E. Matriz de Rigidez de una Viga Empresillada: Aproximación Incluyendo Efectos de Corte. Research Report GADE-RI-2020-01, Universidad Tecnológica Nacional, Facultad Regional Buenos Aires, 2020.

Jouglard C.E. Matriz de Rigidez de una Viga Empresillada: Aproximación Axial Mejorada. Research Report GADE-RI-2021-01, Universidad Tecnológica Nacional, Facultad Regional Buenos Aires, 2021.

Jouglard C.E. and Peker U. Matriz de Rigidez de una Viga Empresillada: Aproximación Flexional Global. Research Report GADE-RI-2019-01, Universidad Tecnológica Nacional, Facultad Regional Buenos Aires, 2019.

Martín H.D. *Utilización de Series de Potencias para la Resolución Económica de Elásticas, Frecuencias y Teoría de Segundo Orden de Entramados de Barras, en el Contexto de la Ingeniería Estructural.* Tesis de Doctorado, Universidad Nacional del Sur, Bahía Blanca, Argentina, 2017.

Maurizi M.J., Bambill E.A., and Martín H.D. Análisis Discreto de Columnas Celosía. *Mecánica Computacional*, 23(5):411–427, 2004.

Noor A.K. Continuum Modeling for Repetitive Lattice Structures. *Applied Mechanics Reviews*, 41(7):285–296, 1988.

Rektorys K. *Variational Methods in Mathematics, Science and Engineering*. D. Raidel Publishing Company, 1980. ISBN 90-277-1060-2.

Wang C.M., Reddy J.N., and Lee K.H. *Shear Deformable Beams and Plates: Relationships with Classical Solutions*. Elsevier, 2000.